

REAL-TIME STABILIZATION AND TRACKING OF A FOUR ROTOR MINI-ROTORCRAFT

P. Castillo, A. Dzul and R. Lozano

Heudiasyc - UTC UMR 6599
Centre de Recherches de Royallieu; B.P. 20529,
60205 Compiègne Cedex, France.
Web page: www.hds.utc.fr/~helico
Telephone: (33) 344234423, Fax: (33) 344234477,
Emails: castillo@hds.utc.fr, dzul@hds.utc.fr, rlozano@hds.utc.fr

Keywords: Aircraft Control, Aircraft Dynamics, Lyapunov Methods, Recursive Control Algorithms.

Abstract

In this paper, we present a controller design and its implementation on a mini-rotorcraft having 4 rotors. The dynamic model is obtained via a Lagrange approach. Experiment results show good performance of the proposed non-linear controller based on nested saturation.

1 Introduction

The automatic control of flying objects has attracted the attention of many researches in the past few years. Generally, the control strategies are based on simplified models which have both a minimum number of states and a minimum number of inputs. These reduced models should retain the main features that must be considered when designing control laws for real aerial vehicles. In this paper we are interested in the design of a relatively simple control algorithm to perform hover and tracking of desired trajectories.

Helicopters are of the most complex flying machines. Its complexity is due to the versatility and manoeuvrability to perform many types of tasks. The classical helicopter is conventionally equipped of a main rotor and a tail rotor. However other type of helicopters exist including the twin rotor (or tandem helicopter) and the co-axial rotor helicopter. In this paper we are particularly interested in controlling a mini-rotorcraft having four rotors.

Four-rotor rotorcraft, like the one shown in figure 1, have some advantages over conventional helicopters. Given that the front and rear motors rotate counter clockwise while the other two rotate clockwise, gyroscopic effects and aerodynamic torques tend to cancel in trimmed flight.

This four rotor rotorcraft does not have a swashplate. In fact it does not need any blade pitch control. The collective input (or throttle input) is the sum of the thrusts of each motor. Pitch movement is obtained by increasing (reducing) the speed of the rear motor while reducing (increasing) the speed of the front motor.

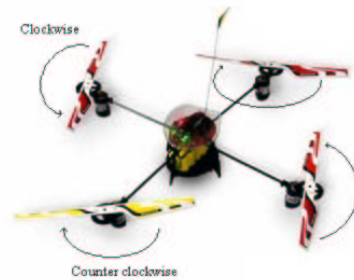


Figure 1: The 4 rotors rotorcraft.

The roll movement is obtained similarly using the lateral motors. The yaw movement is obtained by increasing (decreasing) the speed of the front and rear motors while decreasing (increasing) the speed of the lateral motors. This should be done while keeping the total thrust constant.

In view of its configurations, the four-rotor rotorcraft in figure 1 has some similarities with PVTOL (Planar Vertical Take Off and Landing) aircraft problem. Indeed, if the roll and yaw angles are set to zero, the four-rotor rotorcraft reduces to a PVTOL. In a way the 4-rotor rotorcraft can be seen as two PVTOL aircraft connected such that their axes are orthogonal.

In this paper we present the model of a four-rotor rotorcraft whose dynamical model is obtained via a Lagrange approach. A control strategy is proposed having in mind that the four rotor rotorcraft can be seen as the interconnection of two PVTOL aircraft. Indeed, we first design a control to stabilize the yaw angular displacement. We then control the Pitch movement using a controller based on the dynamic model of a PVTOL (see [6]). Finally, the roll movement is controlled using again a strategy based on the PVTOL.

The control algorithm is based on the nested saturation control strategy proposed by [9]. We prove global stability of the proposed controller. The controller has been implemented on a PC and real time experiments have shown that the proposed control strategy performs well in practice. Robustness with respect to parameter uncertainty and unmodeled dynamics has been ob-

served in a real time application performed by the aerial control team at the University of Technology of Compiègne, France.

The paper is organized as follows: The problem statement is presented in Section 2. Section 3 describes the control law design. In Section 4 we present the experimental results and finally, some conclusions are given in Section 5.

2 Problem statement

In this section we present the model of the four-rotor rotorcraft using a Lagrangian approach. The generalized coordinates describing the rotorcraft position and orientation

$$q = (x, y, z, \psi, \theta, \phi) \in \mathbb{R}^6$$

where (x, y, z) denote the position of the center of mass of the four-rotor rotorcraft relative to the frame \mathcal{I} . (ψ, θ, ϕ) are the three Euler angles (yaw, pitch and roll angles) and represent the orientation of the rotorcraft.

Therefore, the model partitions naturally into translational and rotational coordinates

$$\xi = (x, y, z) \in \mathbb{R}^3, \quad \eta = (\psi, \theta, \phi) \in \mathbb{R}^3$$

The translational kinetic energy of the rotorcraft is

$$T_{\text{trans}} \triangleq \frac{m}{2} \dot{\xi}^T \dot{\xi} \quad (1)$$

where m denotes the mass of the rotorcraft. The rotational kinetic energy is:

$$T_{\text{rot}} \triangleq \frac{1}{2} \dot{\eta}^T \mathbb{J} \dot{\eta} \quad (2)$$

The matrix \mathbb{J} acts as the inertia matrix for the full rotational kinetic energy of the rotorcraft expressed directly in terms of the generalized coordinates η . The only potential energy which needs to be considered is the standard gravitational potential given by

$$U = mgz \quad (3)$$

The Lagrangian representing

$$\begin{aligned} L(q, \dot{q}) &= T_{\text{trans}} + T_{\text{rot}} - U \\ &= \frac{m}{2} \dot{\xi}^T \dot{\xi} + \frac{1}{2} \dot{\eta}^T \mathbb{J} \dot{\eta} - mgz \end{aligned} \quad (4)$$

The model of the full rotorcraft dynamics is obtained from the Euler-Lagrange Equations with external generalized force F

$$\frac{d}{dt} \frac{\partial \mathcal{L}}{\partial \dot{q}} - \frac{\partial \mathcal{L}}{\partial q} = F$$

where $F = (F_\xi, \tau)$ and τ is the generalized moments. F_ξ is the translational force applied to the rotorcraft due to the control inputs. We ignore the small body forces because they are

generally of a much smaller magnitude than the principal control inputs u and τ . We then write:

$$\widehat{F} = \begin{pmatrix} 0 \\ 0 \\ u \end{pmatrix} \quad (5)$$

where (see figure 2)

$$u = f_1 + f_2 + f_3 + f_4$$

and

$$f_i = k_i w_i^2, \quad i = 1, \dots, 4$$

where $k_i > 0$ is a constant and w_i is the angular speed of motor i ($M_i, i = 1, \dots, 4$), then

$$F_\xi = R \widehat{F} \quad (6)$$

where R is the transformation matrix representing the orientation of the rotorcraft. We use c_θ for $\cos \theta$ and s_θ for $\sin \theta$.

$$R = \begin{pmatrix} c_\theta c_\psi & s_\psi s_\theta & -s_\theta \\ c_\psi s_\theta s_\phi - s_\psi c_\phi & s_\psi s_\theta s_\phi + c_\psi c_\phi & c_\theta s_\phi \\ c_\psi s_\theta c_\phi + s_\psi s_\phi & s_\psi s_\theta c_\phi - c_\psi s_\phi & c_\theta c_\phi \end{pmatrix}$$

The generalized forces on the η variables are

$$\tau \triangleq \begin{pmatrix} \tau_\phi \\ \tau_\theta \\ \tau_\psi \end{pmatrix} \quad (7)$$

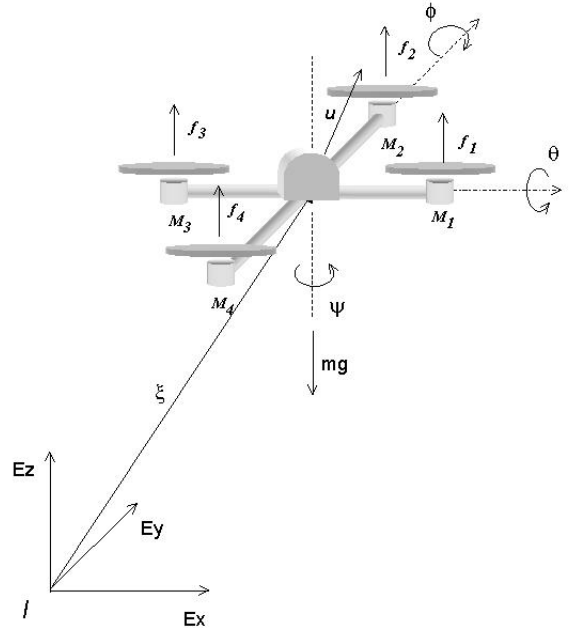


Figure 2: Coordinate system and free-body diagram of the four-rotor rotorcraft.

where

$$\begin{aligned}\tau_\phi &= \sum_{i=1}^4 \tau_{M_i} \\ \tau_\theta &= (f_2 - f_4)\ell \\ \tau_\psi &= (f_3 - f_1)\ell\end{aligned}$$

and where ℓ is the distance from the motors to the center of gravity and τ_{M_i} is the couple produced by motor M_i .

Having obtained the Lagrangian, we observe that it does not contain any cross terms in the kinetic energy combining $\dot{\xi}$ and $\dot{\eta}$ (see (4)), the Euler Lagrange equation can be partitioned into the dynamics for the ξ coordinates and the η dynamics. One obtains

$$m\ddot{\xi} + \begin{pmatrix} 0 \\ 0 \\ mg \end{pmatrix} = F_\xi \quad (8)$$

$$\mathbb{J}\ddot{\eta} + \dot{\mathbb{J}}\dot{\eta} - \frac{1}{2} \frac{\partial}{\partial \eta} (\dot{\eta}^T \mathbb{J} \dot{\eta}) = \tau \quad (9)$$

Defining the Coriolis /Centripetal vector

$$\bar{V}(\eta, \dot{\eta}) = \dot{\mathbb{J}}\dot{\eta} - \frac{1}{2} \frac{\partial}{\partial \eta} (\dot{\eta}^T \mathbb{J} \dot{\eta}) \quad (10)$$

we may write

$$\mathbb{J}\ddot{\eta} + \bar{V}(\eta, \dot{\eta}) = \tau \quad (11)$$

and we can rewrite $\bar{V}(\eta, \dot{\eta})$ as

$$\bar{V}(\eta, \dot{\eta}) = C(\eta, \dot{\eta})\dot{\eta} \quad (12)$$

where $C(\eta, \dot{\eta})$ are referred to as the Coriolis terms. They contain the gyroscopic and centrifugal terms associated with the η dependence of \mathbb{J} .

Finally we obtain

$$m\ddot{\xi} = u \begin{pmatrix} -\sin \theta \\ \cos \theta \sin \phi \\ \cos \theta \cos \phi \end{pmatrix} + \begin{pmatrix} 0 \\ 0 \\ -mg \end{pmatrix} \quad (13)$$

$$\mathbb{J}\ddot{\eta} = -C(\eta, \dot{\eta})\dot{\eta} + \tau \quad (14)$$

3 Control law design

In this section we will develop a control strategy for stabilizing the four-rotor rotorcraft at hover. We will prove global stability of the closed loop system. Furthermore, the proposed controller design is such that the resulting controller is relatively simple and each one of the control inputs can operate in either manual or automatic mode independently. For flight safety reasons this feature is particularly important when implementing the control strategy as will be explained in the section 4. The collective input u in (13) is essentially used to make the altitude reach a desired value. The control input τ_ψ is used to set the yaw displacement to zero. τ_θ is used to control the pitch and

the horizontal movement in the x -axis. Similarly, τ_ϕ is used to control the roll and horizontal displacement in the y -axis.

In order to simplify let us propose a change of the input variables.

$$\tau = C(\eta, \dot{\eta})\dot{\eta} + \mathbb{J}\tilde{\tau} \quad (15)$$

where

$$\tilde{\tau} = \begin{pmatrix} \tilde{\tau}_\psi \\ \tilde{\tau}_\theta \\ \tilde{\tau}_\phi \end{pmatrix} \quad (16)$$

are the new inputs. Then

$$\ddot{\eta} = \tilde{\tau} \quad (17)$$

Rewriting equations (13)-(14):

$$m\ddot{x} = -u \sin \theta \quad (18)$$

$$m\ddot{y} = u \cos \theta \sin \phi \quad (19)$$

$$m\ddot{z} = u \cos \theta \cos \phi - mg \quad (20)$$

$$\ddot{\psi} = \tilde{\tau}_\psi \quad (21)$$

$$\ddot{\theta} = \tilde{\tau}_\theta \quad (22)$$

$$\ddot{\phi} = \tilde{\tau}_\phi \quad (23)$$

where x and y are the coordinates in the horizontal plane, and z is the vertical position (see figure 2). ψ is the yaw angle around the z -axis, θ is the pitch angle around the (new) y -axis, and ϕ is the roll angle around the (new) x -axis. The control inputs u , $\tilde{\tau}_\psi$, $\tilde{\tau}_\theta$ and $\tilde{\tau}_\phi$ are the total thrust or collective input (directed out the bottom of the aircraft) and the new angular moments (yawing moment, pitching moment and rolling moment).

3.1 Altitude and yaw control

The control of the vertical position can be obtained by using the following control input.

$$u = (r_1 + mg) \frac{1}{c_\theta c_\phi} \quad (24)$$

where

$$r_1 = -a_{z_1} \dot{z} - a_{z_2} (z - z_d) \quad (25)$$

a_{z_1} , a_{z_2} are positive constants and z_d is the desired altitude. The yaw angular position can be controlled by applying

$$\tilde{\tau}_\psi = -a_{\psi_1} \dot{\psi} - a_{\psi_2} (\psi - \psi_d) \quad (26)$$

Indeed, introducing (24)-(26) into (18)-(21) and provided that $c_\theta c_\phi \neq 0$, we obtain

$$m\ddot{x} = -(r_1 + mg) \frac{\tan \theta}{\cos \phi} \quad (27)$$

$$m\ddot{y} = (r_1 + mg) \tan \phi \quad (28)$$

$$\ddot{z} = \frac{1}{m} (-a_{z_1} \dot{z} - a_{z_2} (z - z_d)) \quad (29)$$

$$\ddot{\psi} = -a_{\psi_1} \dot{\psi} - a_{\psi_2} (\psi - \psi_d) \quad (30)$$

The control parameters a_{ψ_1} , a_{ψ_2} , a_{z_1} , a_{z_2} should be carefully chosen to ensure a stable well-damped response in the vertical and yaw axes.

From equation (29) and (30) it follows that $\psi \rightarrow \psi_d$ and $z \rightarrow z_d$.

3.2 Roll control (ϕ, y)

Note that from (25) and (29) $r_1 \rightarrow 0$. For a time T large enough, r_1 and ψ are arbitrarily small therefore (27) and (28) reduce to

$$\ddot{x} = -g \frac{\tan \theta}{\cos \phi} \quad (31)$$

$$\ddot{y} = g \tan \phi \quad (32)$$

We will first consider the subsystem given by (23) and (32). We will implement a non-linear controller design based on nested saturations. This type of control allows in the limit a guarantee of arbitrary bounds for $\phi, \dot{\phi}, y$ and \dot{y} . To further simplify the analysis we will impose a very small upper bound on $|\dot{\phi}|$ in such a way that the difference $\tan(\phi) - \phi$ is arbitrarily small. Therefore, the subsystem (23)-(32) reduces to

$$\ddot{y} = g\phi \quad (33)$$

$$\ddot{\phi} = \tilde{\tau}_\phi \quad (34)$$

which represents four integrators in cascade. Then, we propose

$$\tilde{\tau}_\phi = -\sigma_{\phi_1}(\dot{\phi} + \sigma_{\phi_2}(\zeta_{\phi_1})) \quad (35)$$

where $\sigma_i(s)$ is a saturation function such that $|\sigma_i(s)| \leq M_i$ for $i = 0, 1, \dots$ (see the figure 3) and ζ_{ϕ_1} will be defined later to ensure global stability.

We propose the following Lyapunov function

$$V = \frac{1}{2} \dot{\phi}^2. \quad (36)$$

Differentiating V with respect to time, we obtain

$$\dot{V} = \dot{\phi} \ddot{\phi} \quad (37)$$

and from the equation (34) and (35) we have

$$\dot{V} = -\dot{\phi} \sigma_{\phi_1}(\dot{\phi} + \sigma_{\phi_2}(\zeta_{\phi_1})) \quad (38)$$

Note that if $|\dot{\phi}| > M_{\phi_2}$ then $\dot{V} < 0$, that means $\exists T_1$ such that $|\dot{\phi}| \leq M_{\phi_2}$ for $t > T_1$.

We define

$$\nu_1 \equiv \dot{\phi} + \dot{\phi} \quad (39)$$

Differentiating (39)

$$\dot{\nu}_1 = \dot{\phi} + \ddot{\phi} \quad (40)$$

$$= \dot{\phi} - \sigma_{\phi_1}(\dot{\phi} + \sigma_{\phi_2}(\zeta_{\phi_1})) \quad (41)$$

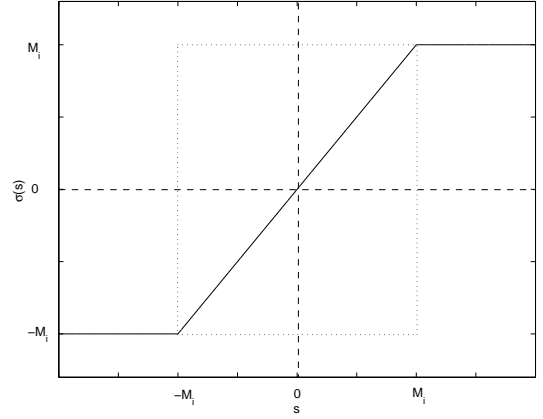


Figure 3: Saturation function

Let us choose

$$M_{\phi_1} \geq 2M_{\phi_2} \quad (42)$$

From the definition of $\sigma(s)$ we can see that $|\sigma_i(s)| \leq M_i$. This implies that in a finite time, $\exists T_1$ such that $|\dot{\phi}| \leq M_{\phi_2}$ for $t \geq T_1$. Therefore, for $t \geq T_1$, $|\dot{\phi} + \sigma_{\phi_2}(\zeta_{\phi_1})| \leq 2M_{\phi_2}$. It then follows that $\forall t \geq T_1$

$$\sigma_{\phi_1}(\dot{\phi} + \sigma_{\phi_2}(\zeta_{\phi_1})) = \dot{\phi} + \sigma_{\phi_2}(\zeta_{\phi_1}) \quad (43)$$

Using (41) and (43), we get

$$\dot{\nu}_1 = -\sigma_{\phi_2}(\zeta_{\phi_1}) \quad (44)$$

Let us define

$$\zeta_{\phi_1} \equiv \nu_1 + \sigma_{\phi_3}(\zeta_{\phi_2}) \quad (45)$$

Introducing the above in (44) it follows

$$\dot{\nu}_1 = -\sigma_{\phi_2}(\nu_1 + \sigma_{\phi_3}(\zeta_{\phi_2})) \quad (46)$$

The upper bounds are assumed to satisfy

$$M_{\phi_2} \geq 2M_{\phi_3} \quad (47)$$

This implies that $\exists T_2$ such that $|\nu_1| \leq M_{\phi_3}$ for $t \geq T_2$. From equation (39) we can see that $\forall t \geq T_2$, $|\dot{\phi}| \leq M_{\phi_3}$. M_{ϕ_3} should be chosen small enough such that $\tan \phi \approx \phi$.

From (46) and (47), we have that for $t \geq T_2$, $|\nu_1 + \sigma_{\phi_3}(\zeta_{\phi_2})| \leq 2M_{\phi_3}$. It then follows that, $\forall t \geq T_2$

$$\sigma_{\phi_2}(\nu_1 + \sigma_{\phi_3}(\zeta_{\phi_2})) = \nu_1 + \sigma_{\phi_3}(\zeta_{\phi_2}) \quad (48)$$

Introducing the following function

$$\nu_2 \equiv \nu_1 + \dot{\phi} + \frac{\dot{y}}{g} \quad (49)$$

then

$$\dot{\nu}_2 = \dot{\nu}_1 + \dot{\phi} + \frac{\ddot{y}}{g} \quad (50)$$

Using (33), (39), (46) and (48) into (50), we obtain

$$\dot{\nu}_2 = -\sigma_{\phi_3}(\zeta_{\phi_2}) \quad (51)$$

Now, define ζ_{ϕ_2} as

$$\zeta_{\phi_2} \equiv \nu_2 + \sigma_{\phi_4}(\zeta_{\phi_3}) \quad (52)$$

Let us rewrite (51) as

$$\dot{\nu}_2 = -\sigma_{\phi_3}(\nu_2 + \sigma_{\phi_4}(\zeta_{\phi_3})) \quad (53)$$

We chose

$$M_{\phi_3} \geq 2M_{\phi_4} \quad (54)$$

We then have that in a finite time, $\exists T_3$ such that $|\nu_2| \leq M_{\phi_4}$ for $t \geq T_3$, this implies from (49) that \dot{y} is bounded.

For $t \geq T_3$, $|\nu_2 + \sigma_{\phi_4}(\zeta_{\phi_3})| \leq 2M_{\phi_4}$. It then follows that, $\forall t \geq T_3$

$$\sigma_{\phi_3}(\nu_2 + \sigma_{\phi_4}(\zeta_{\phi_3})) = \nu_2 + \sigma_{\phi_4}(\zeta_{\phi_3}) \quad (55)$$

Defining

$$\nu_3 \equiv \nu_2 + 2\frac{\dot{y}}{g} + \phi + \frac{y}{g} \quad (56)$$

then

$$\dot{\nu}_3 = \dot{\nu}_2 + 2\frac{\ddot{y}}{g} + \dot{\phi} + \frac{\dot{y}}{g} \quad (57)$$

Finally using (33), (48), (53) and (55) into (57), we obtain

$$\dot{\nu}_3 = -\sigma_{\phi_4}(\zeta_{\phi_3}) \quad (58)$$

We propose ζ_{ϕ_3} of the following form

$$\zeta_{\phi_3} \equiv \nu_3 \quad (59)$$

then

$$\dot{\nu}_3 = -\sigma_{\phi_4}(\nu_3) \quad (60)$$

this implies that $\nu_3 \rightarrow 0$. From (53) it follows that $\nu_2 \rightarrow 0$ and from equation (52) $\zeta_{\phi_2} \rightarrow 0$. From (46) $\nu_1 \rightarrow 0$ then from (45) $\zeta_{\phi_1} \rightarrow 0$.

We can see from equation (38) that $\dot{\phi} \rightarrow 0$. From equation (39) we get $\phi \rightarrow 0$. From (49) $\dot{y} \rightarrow 0$ and finally from (56) $y \rightarrow 0$.

Using (39), (45), (49), (52), (56) and (59), we can rewrite equation (35) as

$$\begin{aligned} \tilde{\tau}_\phi = & -\sigma_{\phi_1}(\dot{\phi} + \sigma_{\phi_2}(\phi + \dot{\phi} + \\ & \sigma_{\phi_3}(2\phi + \dot{\phi} + \frac{\dot{y}}{g} + \\ & \sigma_{\phi_4}(\dot{\phi} + 3\phi + 3\frac{\dot{y}}{g} + \frac{y}{g})))) \end{aligned} \quad (61)$$

3.3 Pitch control (θ, x)

From equations (33) and (61) we obtain $\phi \rightarrow 0$. (31) gives

$$\ddot{x} = -g \tan \theta \quad (62)$$

We take the sub-system

$$\ddot{x} = -g \tan \theta \quad (63)$$

$$\ddot{\theta} = \tilde{\tau}_\theta \quad (64)$$

As before, we assume that the control strategy will insure a very small bound on $|\theta|$ in such a way that $\tan \theta \approx \theta$. Therefore (63) reduces to

$$\ddot{x} = -g\theta \quad (65)$$

Using a procedure similar to the one proposed for the roll control, we obtain

$$\begin{aligned} \tilde{\tau}_\theta = & -\sigma_{\theta_1}(\dot{\theta} + \sigma_{\theta_2}(\theta + \dot{\theta} + \\ & \sigma_{\theta_3}(2\theta + \dot{\theta} - \frac{\dot{x}}{g} + \\ & \sigma_{\theta_4}(\dot{\theta} + 3\theta - 3\frac{\dot{x}}{g} - \frac{x}{g})))) \end{aligned} \quad (66)$$

4 Experimental results

In this section we present the experimental results, we describe the hardware used and explain the experiment.

4.1 Hardware

The flying machine we have used is a mini-robotcraft having four rotors manufactured by Draganfly Innovations Inc., (<http://www.rctoys.com>). The radio is a Futaba Skysport 4. The radio and the PC (INTEL Pentium 3) are connected using data acquisition cards (ADVANTECH PCL-818HG and PCL-726). In order to simplify the tuning of the controller and for flight security reasons, we have introduced several switches in the PC-radio interface so that each control input can operate either in manual mode or in automatic control mode.

The connection in the radio is directly made to the joystick potentiometers for the gas, yaw, pitch and roll controls. The robotcraft evolves freely in a 3D space without any flying stand.

We use the 3D tracker system (POLHEMUS) [5] for measuring the position (x,y,z) and orientation (ψ, θ, ϕ) of the robotcraft. The Polhemus is connected via RS232 to the PC.

4.2 Experiment

With respect to the time derivatives, we have simplified the mathematical computation by setting

$$\dot{q}_t = \frac{q_t - q_{t-T}}{T} \quad (67)$$

where q is a given variable and T is the sampling period. In the experiment $T = \frac{1}{14} s$.

The gain values used for the control law are $a_{\psi_1} = 2.374$, $a_{\psi_2} = 0.08$, $a_{z_1} = 0.001$, $a_{z_2} = 0.002$, $M_{\theta_1} = 2$, $M_{\theta_2} = 1$, $M_{\theta_3} = 0.2$, $M_{\theta_4} = 0.1$, $M_{\phi_1} = 2$, $M_{\phi_2} = 1$, $M_{\phi_3} = 0.2$ and $M_{\phi_4} = 0.1$.

The control objective is to make the mini-robotcraft hover at an altitude of 30 [cm] i.e. we wish to reach the position $(x, y, z) = (0, 0, 30 [cm])$ while $(\psi, \theta, \phi) = (0, 0, 0)$. We also make the rotorcraft follow a simple horizontal trajectory.

Figure 4 and 5 show the performance of the controller when applied to the rotorcraft. Videos of the experiments can be seen in the following address: http://www.hds.utc.fr/~castillo/4r_fr.html

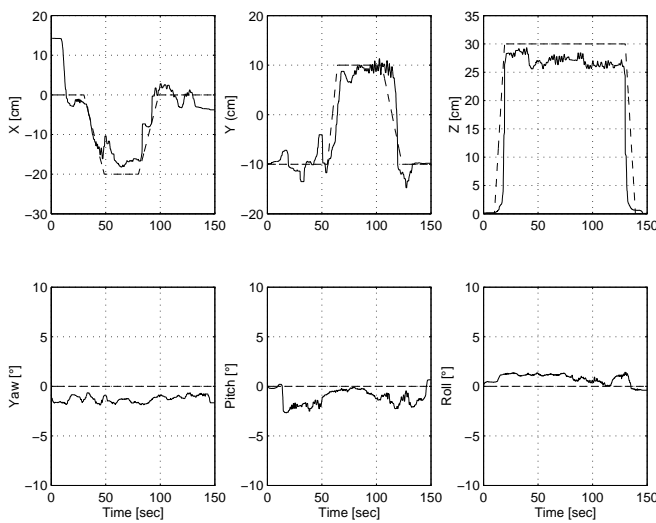


Figure 4: Position (x, y, z) and orientation (ψ, θ, ϕ) of the four rotorcraft. The dotted lines represent the derived trajectories.

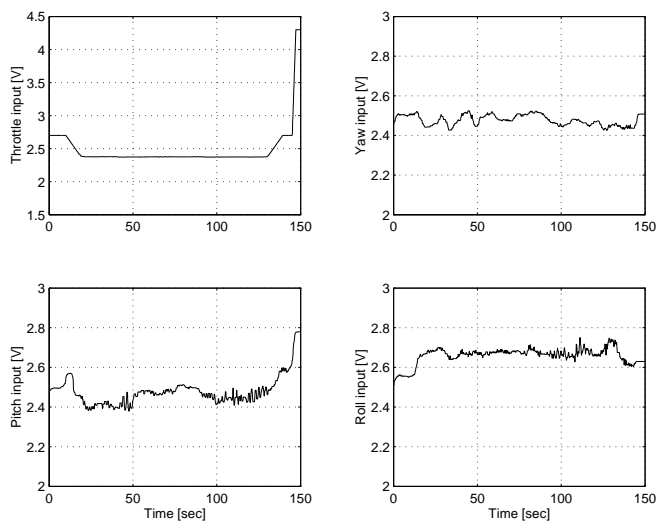


Figure 5: Controls inputs (throttle input, yaw, pitch and roll)

5 Conclusion

We have proposed a stabilization control algorithm for a mini-robotcraft having four rotors. The dynamic model of the rotorcraft was obtained via a Lagrange approach and the proposed control algorithm is based on nested saturations.

The proposed strategy has been successfully applied to the rotorcraft, and the experimental results have shown that the controller performs satisfactorily.

To the best of our knowledge, this is the first successful real-time control applied to a four-rotor rotorcraft.

References

- [1] T. S. Alderete, Simulator aero model implementation, NASA Ames Research Center, Moffett Field, California.
- [2] W. Barnes McCormick, *Aerodynamics Aeronautics and Flight Mechanics*, John Wiley & Sons, INC., New York, 1995.
- [3] B. Etkin, *Dynamics of Flight*, John Wiley and Sons, Inc., New York, 1959.
- [4] I. Fantoni, R. Lozano, *Control of nonlinear mechanical underactuated systems*. Springer-Verlag, Communications and Control Engineering Series, 2001.
- [5] Fastrack 3Space Polhemus, *User's Manual*, Colchester, Vermont, USA.
- [6] J. Hauser, S. Sastry & G. Meyer, Nonlinear control design for slightly nonminimum phase systems: Application to V/STOL aircraft, *Automatica*, 28(4):665-679, 1992.
- [7] R. Lozano, B. Brogliato, O. Egeland, B. Maschke. *Passivity-based control system analysis and design*. Springer-Verlag, Communications and Control Engineering Series, 2000. ISBN 1-85233-285-9.
- [8] L. Marconi, A. Isidori, A. Serrani, Autonomous vertical landig on an oscillating platform: an internal-model based approach, *Automatica*, 38: 21-32, 2002.
- [9] A. R. Teel, Global stabilization and restricted tracking for multiple integrators with bounded controls, *Systems and Control Letters*, 1992.